Geophysical Research Letters

Key Points:
- Observational evidence of a basin-wide gyre reversal in the Gulf of Taranto, anticyclonic in October 2014 and cyclonic in June–July 2016
- Long-term satellite analysis suggests that, in the period from 1992–2018, cyclonic are more frequent than anticyclonic gyres
- Gyre currents undergo instabilities and formation of submesoscale and mesoscale eddies at the outer rim of the gyres

Correspondence to:
I. Federico,
ivan.federico@cmcc.it

Observational Evidence of the Basin-Wide Gyre Reversal in the Gulf of Taranto

I. Federico[1] , N. Pinardi[1,2] , V. Lyubartsev[1] , F. Maicu[2,3], S. Causio[1] , F. Trotta[2], C. Caporale[4], G. Coppini[1] , M. Demarte[4], A. Falconieri[5] , T. Lacava[5] , R. Lecci[1] , M. Lisi[2], G. Lorenzetti[3], G. Manfè[3], A. A. Sepp-Neves[2], and L. Zaggia[6]

[1]Euro-Mediterranean Center on Climate Change (CMCC), Lecce, Italy, [2]Department of Physics and Astronomy, University of Bologna, Bologna, Italy, [3]National Research Council, Institute of Marine Science, Venice, Italy, [4]Hydrographic Institute of Italian Navy, Genoa, Italy, [5]National Research Council, Institute of Methodologies for Environmental Analysis, Tito Scalo (Potenza), Italy, [6]National Research Council, Institute of Geosciences and Earth Resources, Padova, Italy

Abstract The paper shows for the first time the observational evidence of basin-wide gyre reversal in the Gulf of Taranto (north-western Ionian Sea in the eastern Mediterranean Sea) by means of two specifically designed in situ oceanographic campaigns (based on CTD and ADCP measurements). The analysis of the in situ data shows a change in circulation from anticyclonic in October 2014 to cyclonic in June–July 2016. Furthermore, long-term (1993–2018) analysis using gridded satellite altimetry data in the Gulf of Taranto shows that the cyclonic gyres are more frequent than anticyclonic gyres. The latter occur only for 2 to 3 years at a time in some decades.

Plain Language Summary The work shows the observational evidence of a phenomenon named gyre reversal (the circulation changes from cyclonic to anticyclonic), occurring in ocean regions with specific geometry characteristics, among others the Gulfs. In particular, our results unequivocally show for the first time the reversal of the basin-scale gyre circulation in the Gulf of Taranto (north-western Ionian Sea in the eastern Mediterranean Sea), by means of in situ oceanographic measurements and satellite data.

1. Introduction

The reversal of basin-wide gyres in the world ocean can be modulated by the specific basin geometric characteristics (e.g., open ocean versus semienclosed seas and gulfs), changes in wind direction, and the water mass transformation and spreading processes. Some of the most well-known basin-scale gyre reversals occur in open ocean areas (Somali current system, Schott & Fischer, 2000, and Prasad & Ikeda, 2002; Bay of Bengal, Eigenheer & Quadfasel, 2000; Beaufort Sea, Preller & Posey, 1989; Northern Ionian Sea, Borzelli et al., 2009, Pinardi et al., 2015, and Rubino et al., 2020) and semienclosed seas and Gulfs (Red Sea, Yao et al., 2014a, 2014b; Gulf of Finland, Liblik et al., 2013; Gulf of California, Carrillo et al., 2002, and Marinone, 2003; Sulu Sea in the Philippine Archipelago, Han et al., 2009; Panama Bight, Devis-Morales et al., 2008; and the South China Sea, Wu et al., 1998, and Fang et al., 2002).

Our study aims to discover the reversal of a basin-scale gyre in the Gulf of Taranto, which is located in the north-western Ionian Sea (Figure 1). The Gulf of Taranto is a semienclosed ocean area, covering about 16,300 km^2 (Ciancia et al., 2018) and including the coasts of the Italian regions of Apulia, Basilicata, and Calabria. It is connected to the northern Ionian Sea and the eastern Mediterranean Sea by an extended section, the Gulf of Taranto Boundary Section (GT-BS in Figure 1), which includes a narrow trench deeper than 2,000 m. The continental shelf area, defined as the area shallower than 200 m, covers only 10% of the total Gulf area. Wider shelves are present on the eastern side (Apulia) and five main rivers (Bradano, Basento, Agri, Sinni, and Crati) discharge from the western coastline with a relative low annual mean runoff (~75 m^3/s, Verri et al., 2018).

The only basin-scale survey mapping the vertical and horizontal structure of the temperature and salinity fields for the entire Gulf of Taranto was analyzed by Pinardi et al. (2016). The basin-scale circulation was found to be characterized by an anticyclonic gyre with a rim current which undergoes instabilities and forms submesoscale structures (Trotta et al., 2017). Pinardi et al. (2016) highlighted that the Gulf of Taranto is
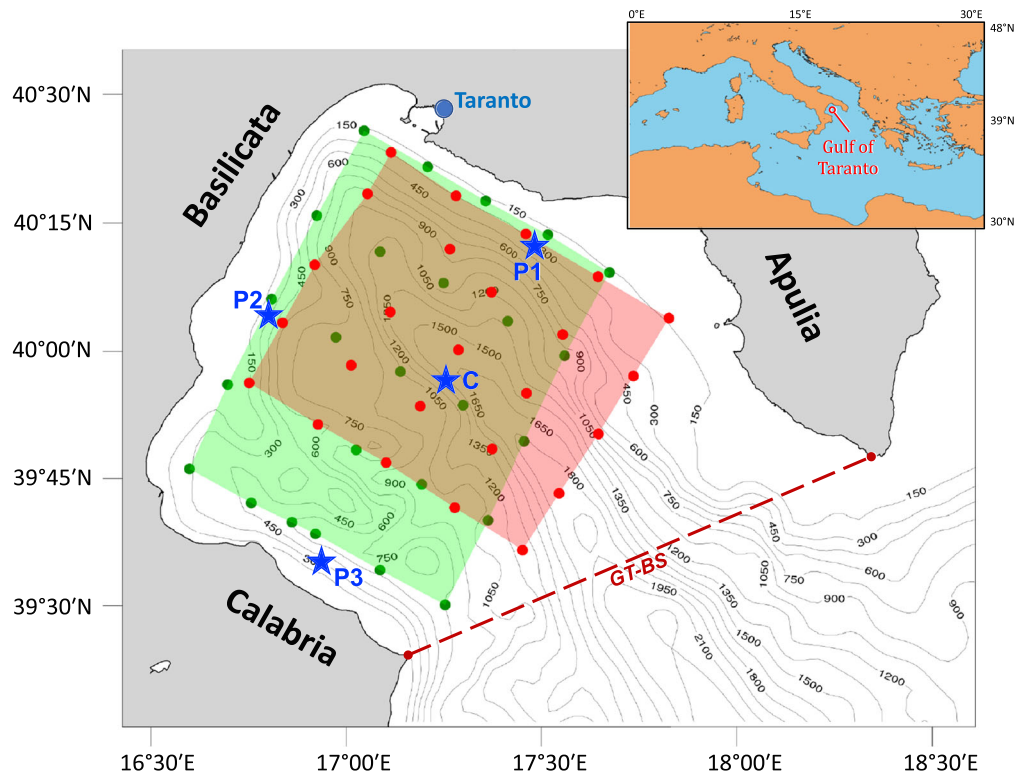
Figure 1. The Gulf of Taranto coastlines and bathymetry. Shaded areas with red and green points refer to the distribution of sampling stations during the October 2014 (MREA14) and June–July 2016 (MREA16) cruises, respectively (see section 2). Blue stars refer to center and peripheral points for the calculation of basin-scale gyre index (see section 3). The GT-BS dashed line indicates the Gulf of Taranto Boundary Section.

characterized by (i) a mixed layer thickness extending down to 30 m in late summer; (ii) an intermediate water salinity maximum—indicative of Modified Levantine Intermediate Waters—in the deep part of the Gulf; and (iii) low salinity values at the surface indicating surface waters of Adriatic or Atlantic origin.

Federico et al. (2017) simulated the basin-scale circulation of the Gulf of Taranto using a high-resolution operational forecasting model for the southern Adriatic and northern Ionian Sea area. The simulated Gulf of Taranto circulation structure is affected by the Western Adriatic Coastal Current (WACC) position and strength (Artegiani et al., 1997a, 1997b; Ciancia et al., 2018; Cushman-Roisin et al., 2001). The WACC normally flows southward out of the Adriatic Sea, entering the Gulf of Taranto from the surface down to 100 m. During October 2014 the WACC was weak and a reversed, northeastward coastal current was present along the Apulia coasts, exiting the GT-BS, thus allowing for a basin-wide anticyclonic circulation to form.

On the basis of a long-term modeling reanalysis, Pinardi et al. (2016) discussed a possible reversal of the basin-scale anticyclonic gyre of the Gulf of Taranto, connecting this feature to the inflow-outflow system of the GT-BS. However, the evidence was not conclusive because the lack of in situ observational data for the Gulf of Taranto made the reanalysis little more than a simulation.

Here we show for the first time the observational evidence of gyre reversal in the Gulf of Taranto in June–July 2016 by means of (i) two specifically planned high-resolution in situ surveys composed by synoptic station distributions, designed on the basis of Marine Rapid Environmental Assessment (MREA) concepts (Frolov et al., 2014; Lermusiaux, 2007; Robinson & Sellschopp, 2002); and (ii) the analysis of gridded satellite altimetry. We compare the emerging basin-scale circulation with the already published survey in October 2014 (Pinardi et al., 2016). Our results unequivocally show the reversal of the basin-scale gyre circulation in the Gulf of Taranto. Furthermore, the 26-year long time series from satellite altimetry allows us to determine the frequency of the reversals.

Section 2 discusses the in situ surveys and makes comparisons with past investigations. Section 3 analyzes the satellite data. The discussion and conclusions are reported in section 4.

2. The Gyre Reversal From In Situ Data

The MREA strategy uses a uniform sampling to cover the area of interest within synoptic time scales. In our analysis we use surveys carried out in 1–11 October 2014 (known as MREA14) and in 27 June to 7 July 2016 (MREA16). Each of the MREA surveys are repeated twice to confirm the emerging pattern from the sampling and to verify modeling forecast results (e.g., Federico et al., 2017). In both MREA14 and MREA16, the vertical sampling was carried out by means of CTD stations profiling the water column at 1 m resolution and measuring the temperature and salinity down to a maximum depth of 400 m in order to map the upper thermocline of this area.

MREA14 is detailed in Pinardi et al. (2016) and its sampling is shown in the red shaded area in Figure 1. The mean spacing between stations (~16 km) is approximately the Rossby radius of deformation for the eastern Mediterranean (Hecht et al., 1998). This distance was chosen as a good compromise between the time to cover the entire Gulf synoptically and the required spatial resolution. The mapping of the near-surface geostrophic circulation showed the presence of an anticyclonic basin-scale gyre occupying the central open-sea area of the Gulf of Taranto.

The second experiment, MREA16, which is analyzed here for the first time, repeated the MREA14 experiment and investigated a possible reversal of the anticyclonic circulation. The sampling methodology tested in 2014 was strengthened by integrating the classical CTD data collection with additional simultaneous direct measurements of currents, by means of a vessel-mounted ADCP measuring the current speed and direction in the surface layer, down to a depth of 20 m. The sampling scheme with the position of stations is highlighted by the shaded area with green points in Figure 1. The MREA16 measurements were carried out with an Idronaut CTD 316Plus and ADCP Teledyne RD Rio Grande 600 khz on board of the ARETUSA-5304 hydro-oceanographic Research Vessel of the Italian Navy Hydrographic Institute.

As with MREA14, the second survey (MREA16) consisted of two legs (LS1, 27–30 June 2016, and LS2, 4–7 July 2016) with the same station positions and a time difference of about a week. The mean spacing between stations was slightly greater (~18 km) than in MREA14, in order to cover a wider Gulf area (e.g., the southern shelf-coastal zone of Gulf in front of Calabria not covered by MREA14) again in a synoptic time framework.

The ADCP velocity profiles were mapped by means of an objective analysis (Bretherton et al., 1976; Carter & Robinson, 1987), described in detail in Appendix A of Pinardi et al. (2016). The components of the measured velocity field were mapped separately. Detiding of ADCP data were neglected due to the microtidal regime of the basin (tidal range of 20 cm as reported in Federico et al., 2017).

Figure 2 shows the ADCP circulation from LS1, LS2, and LS1 + LS2 (average vertical velocity profiles of the two legs) at 5 and 20 m, highlighting the following features: (i) a well-defined cyclonic circulation at the basin scale both for LS1 and LS2; (ii) a cyclonic rim current composed of intensified jets; (iii) two smaller scale cyclonic vortices, enclosed within the basin-scale gyre in LS1 and LS2; (iv) a decrease of circulation intensity between LS1 and LS2.

CTD data collected in MREA14 and MREA16 have been analyzed in Figure 3 showing the density profiles (Figure 3a) and the dynamic height and geostrophic currents (Figures 3b–3c). The horizontal-average density profiles show the deep autumn mixed layer extending down to 30 m for MREA14, typical of the Mediterranean Sea (Hecht et al., 1998) and in MREA16, the stratification characterizing the warming during summer seasons.

The density profiles were used to construct the dynamic height at 5 m with respect to a reference level of 100 m, using again the same objective analysis mapping techniques. This shallow no-motion level was chosen in order to capture part of the connections between the open ocean and the shelf, and to use all the stations on the shelf, since some of these stations were sampled down to a depth of only 100 m. Using a deeper level of no-motion does not change the structure of the gyre, only its amplitude, as expected. The dynamic height and the derived geostrophic currents (vectors overlapped) are displayed in Figures 3b–3c for the MREA14 and MREA16.
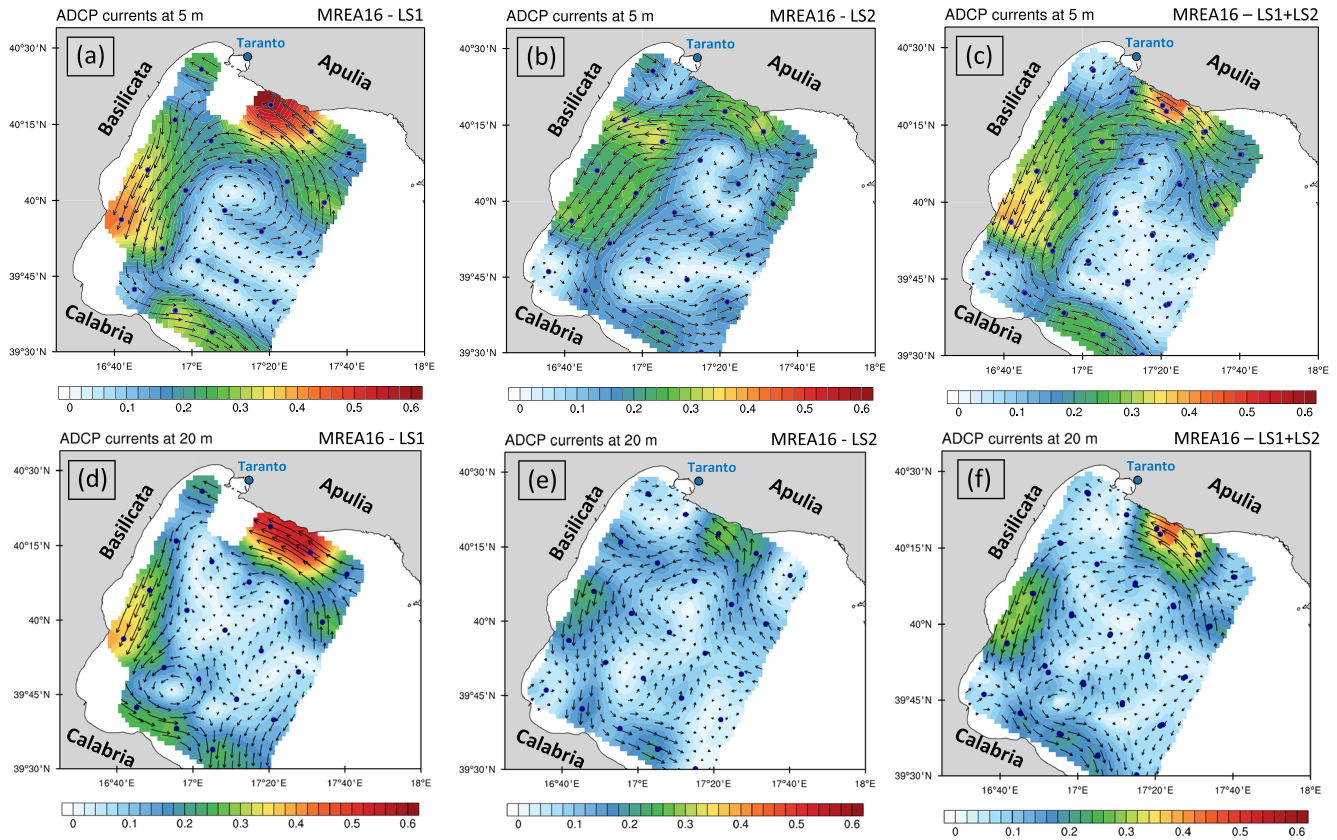
Figure 2. MREA16 maps of ADCP-measured circulation for LS1 (a and d), LS2 (b and e), and LS1 + LS2 (c and f) at 5 and 20 m. Colors indicate the velocity magnitude.

The 2014 anticyclonic gyre has been replaced by a cyclonic structure in 2016. The periphery of the gyres is characterized by a rim current and at the outer side of the rim current cyclonic eddies (E1 and E2 in Figures 3b–3c for MREA14) and a warm core eddy (E3 for MREA16) are present. The E2 eddy has been classified as a submesoscale eddy and its process of formation explained with a mixed barotropic-baroclinic instability of the rim current (Trotta et al., 2017).
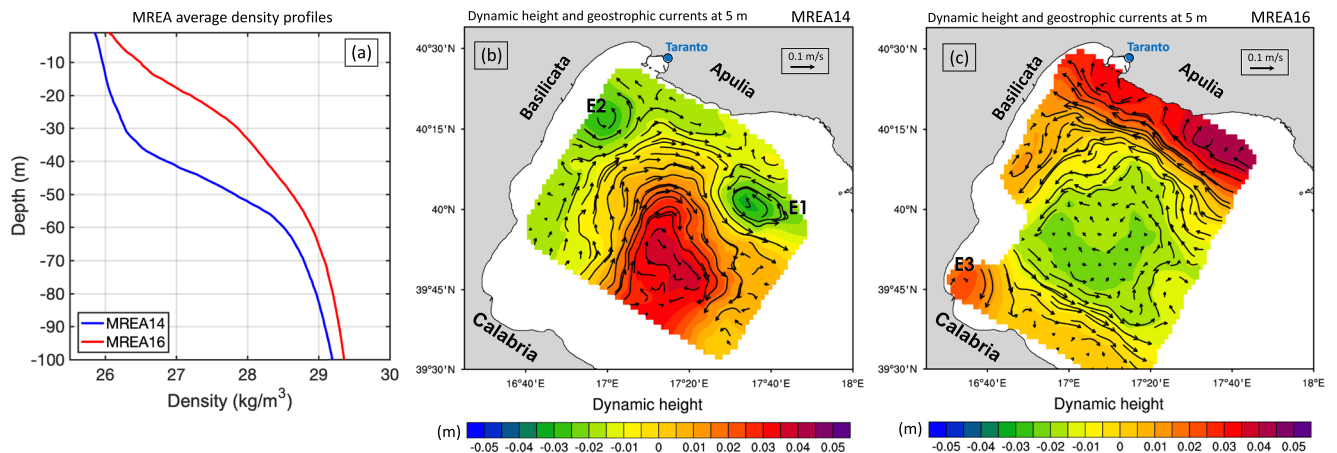
Figure 3. Horizontal average density profiles for MREA14 and MREA16 (a). Dynamic height and geostrophic circulation (vectors overlapped) at 5 m with respect to the 100 m reference level for MREA14 (b) and MREA16 (c). The vertical profiles and the dynamic height are calculated from the two legs average (LS1 + LS2) of the temperature and salinity profiles. E1 and E2 in (c) indicate cyclonic eddies, E3 anticyclonic eddy.
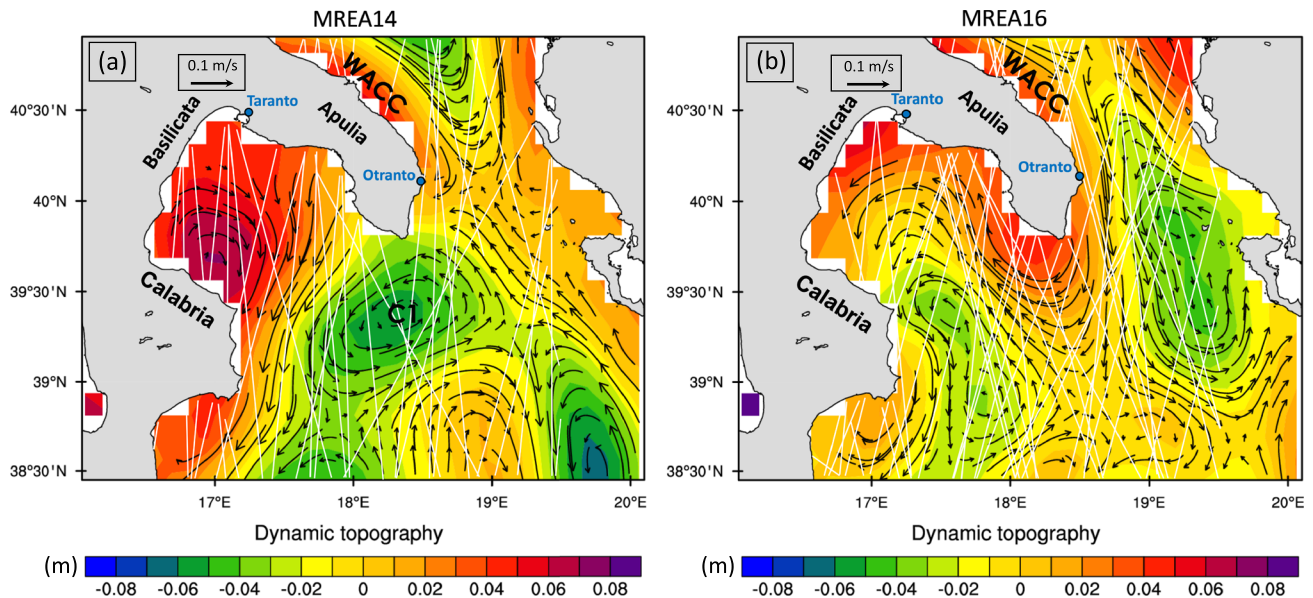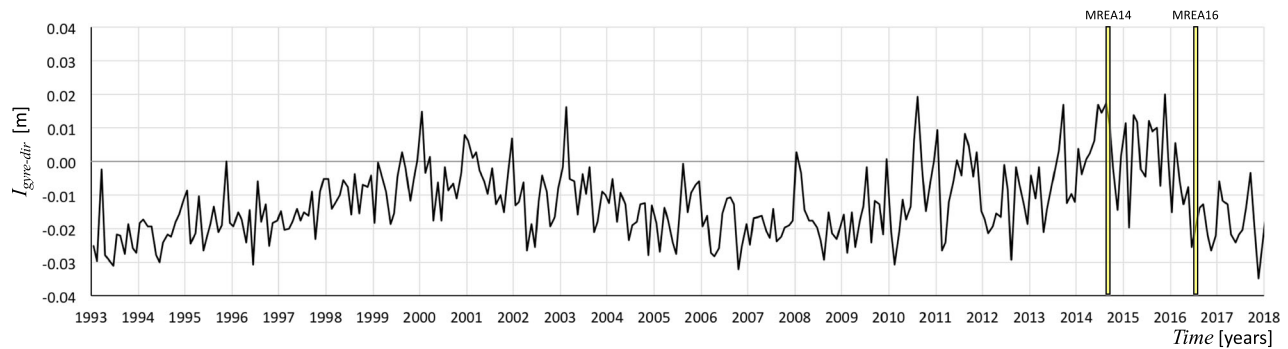
Figure 4. Maps of absolute dynamic topography by satellite (CMEMS products: SEALEVEL_MED_PHY_L4_REP_OBSERVATIONS_008_051) and geostrophic circulation (vectors overlapped) for the period (a) 1–11 October 2014 (MREA14) and (b) 27 June to 7 July 2016 (MREA16). White lines indicate the tracks of satellite (CMEMS products: SEALEVEL_EUR_PHY_L3_REP_OBSERVATIONS_008_061) for the two MREA surveys.

3. The Gyre Reversal From Satellite Altimetry

After the analysis of the in situ data, we used satellite data to assess the likelihood of the Gulf of Taranto basin-scale gyre reversals in the past 26 years (1993–2018). The satellite altimeter data provided by the Copernicus Marine Environment Monitoring Service (CMEMS) (http://marine.copernicus.eu/) are used to investigate the circulation patterns in the Gulf of Taranto. We used the combined altimetry CMEMS L4 products (SEALEVEL_MED_PHY_L4_REP_OBSERVATIONS_008_051) for 1993–2018, which integrate data from all altimeter missions interpolated onto a uniform grid with a horizontal resolution of $1/8° \times 1/8°$. The variables are the absolute dynamic topography (ADT) and the absolute surface geostrophic velocities. A full description of the satellite products is available in the Sea Level Product User Manual (http://marine.copernicus.eu/documents/PUM/CMEMS-SL-PUM-008-032-062.pdf), in the Quality information Document (http://marine.copernicus.eu/documents/QUID/CMEMS-SL-QUID-008-032-062.pdf), as well as in Taburet et al. (2019).

First, we averaged the satellite data in the same period as the two in situ surveys. Figures 4a and 4b show the ~10-day-averaged maps of ADT and associated surface geostrophic currents for 2014 and 2016. As expected from the in situ surveys, the Gulf of Taranto shows a reversal of the basin-scale circulation from anticyclonic in 2014 to cyclonic in 2016. Overall, the circulation reversal is evident and similar between satellite altimetry maps and in situ surveys MREA14 and MREA16. Although the strength of the satellite ADT high and lows and the dynamic height from in situ data (Figures 3b–3c) are similar, they are different in several key ways. In particular, the satellite data show the anticyclonic gyre in MREA14 displaced with respect to the in situ observations and the cyclonic circulation in MREA16 is displaced south-west with respect to Figure 2. We argue that this is due to the satellite track sampling scheme and the coarseness of the mapping grid. These differences could be also explained by the mapping procedure of the gridded satellite altimetry described in Pujol et al. (2016). In fact, the L4 satellite data are mapped from L3 tracks, indicated by white lines in Figure 4, using a procedure based on a time-period spanning (~±15 days at 40°N) with respect to the reference day. Furthermore, the differences between satellite and in situ data could also be due to the type of objective analysis correlation parameters (Ducet et al., 2000; Le Traon et al., 1998). Thus, the satellite features might be displaced with respect to the in situ survey due to the temporal and spatial averaging window of the satellite objective analysis.

Figure 5. Basin-scale gyre-direction index in the Gulf of Taranto calculated from satellite absolute dynamic topography from gridded satellite altimetry data from 1993 to 2018. Yellow boxes highlight the MREA14 and MREA16 time periods.

The basin-scale coverage of the satellite maps allows us to speculate on the possible mechanisms of reversal due to the differences in flow field across the GT-BS and in the Northern Ionian. During MREA14, the Northern Ionian offshore area was dominated by a basin-scale cyclonic eddy, indicated as C1 in Figure 4a. The WACC, normally flowing along the Apulia coasts, was weak and did not exit the Adriatic Sea. On the contrary, during MREA16 (Figure 4b), the WACC was strong and flowing around the Apulia peninsula, entering the Gulf of Taranto and feeding the cyclonic circulation. We argue that the different Northern Ionian eddies/gyres in the 2 years change the inflow/outflow conditions across the GT-BS, thus affecting the Gulf of Taranto circulation. The Northern Ionian gyres change the intrusion of the WACC in the Gulf of Taranto thus affecting the basin-scale circulation.

In order now to analyze the possibility of such reversals in the satellite time period, we devised a basin-scale gyre index, defined as

$$I_{gyre-dir} = ADT_C - (ADT_{P1} + ADT_{P2} + ADT_{P3})/3, \tag{1}$$

where ADT refers to the absolute dynamic topography, and the subscripts C, P1, P2, and P3 to the relative ADT at the center and the periphery points at the bathymetric isoline of 300 m, as reported in Figure 1 (blue stars). Positive values of $I_{gyre-dir}$ indicate an anticyclonic-oriented gyre, and negative values indicate a cyclonic pattern. The robustness of $I_{gyre-dir}$ was tested varying the position of the peripheral points following the 300 m bathymetric isoline and using a spacing of 10 km between them. Results were substantially identical to the one obtained using the three points indicated by blue stars in Figure 1.

Figure 5 shows the monthly mean time series of $I_{gyre-dir}$ from 1993 to 2018, highlighting a low frequency, decadal to interannual gyre variability and reversal events. Looking in detail at the entire time series, the circulation is mostly cyclonic with three reversals: one between 2000 and 2003, 2010 and 2012, and the last 2014 and 2015. For the whole of 2015, the circulation reverses with a very high frequency (seven times in a year) and then it returns to cyclonic from 2016 until 2018. The $I_{gyre-dir}$ negative values (up to ~−0.03 m) are larger in absolute value than the positive values (~ + 0.02 m), indicating that the anticyclonic circulation is weaker than its cyclonic counterpart.

The decadal variability of the index is also noticeable in Figure 5. This slow time component is probably connected to long-term atmospheric forcing variability (Demirov & Pinardi, 2002; Pinardi et al., 1997) and its remote response in the different parts of the basin.

4. Discussion and Conclusions

Using two specifically designed basin-scale in situ surveys, we have demonstrated for the first time the observational evidence of basin-scale gyre reversal in the Gulf of Taranto. The dynamic height built upon the CTD data collection depicted a change in basin-scale circulation from anticyclonic in 2014 to cyclonic in 2016. In 2016 the surface currents were also mapped by ADCPs in the first 20 m of the water column confirming that the upper layer circulation was cyclonic.

Both mesoscale and submesoscale eddies, cyclonic and anticyclonic, appear at the outer rim of the Gulf of Taranto gyres. Given that at the border of anticyclonic gyres there is upwelling while downwelling is prevalent in the cyclonic case, it is clear that the Gulf of Taranto gyre basin circulation reversal could be crucial in terms of ecosystem variability and changes. This correlation should be explored in the future. For instance, the reversal of the Gulf of Taranto gyre occurred during the late 2010 and beginning 2011 (Figure 5) have been connected to an anomalous chlorophyll-a bloom in the GT, as described in Ciancia et al. (2018).

The satellite ADT was found to be consistent with the in situ dynamic height in 2014 and 2016, thus enabling us to use the whole 26-year satellite altimetry data to define an index of the Gulf of Taranto gyre reversal. The index shows that the basin-scale circulation is dominated by cyclonic basin-scale gyres, with reversals occurring only 10–15 times for the entire 26 years period. The basin-scale circulation of the adjacent basins, the WACC, and the Northern Ionian eddies/gyres could be responsible for driving such episodic changes through the Gulf of Taranto-Boundary Section.

Future physical modeling studies in the Gulf of Taranto should focus on the role played by atmospheric forcing conditions together with the lateral boundary conditions to force the Gulf of Taranto reversal, the decadal variability, and the coupling with biogeochemistry to assess the ecosystem impact of the basin scale variability.

Data Availability Statement

The in situ data can be downloaded in ascii online (https://mrea.sincem.unibo.it/index.php/experiments/mrea16). Please contact nadia.pinardi@unibo.it for further information.

References

Artegiani, A., Bregant, D., Paschini, E., Pinardi, N., Raicich, F., & Russo, A. (1997a). The Adriatic Sea general circulation. Part I: Air-sea interactions and water mass structure. *Journal of Physical Oceanography*, 27, 1492–1514.

Artegiani, A., Bregant, D., Paschini, E., Pinardi, N., Raicich, F., & Russo, A. (1997b). The Adriatic Sea general circulation. Part II: Baroclinic circulation structure. *Journal of Physical Oceanography*, 27, 1515–1532.

Borzelli, G. L. E., Gačić, M., Cardin, V., & Civitarese, G. (2009). Eastern Mediterranean Transient and reversal of the Ionian Sea circulation. *Geophysical Research Letters*, 36, 69–72. https://doi.org/10.1029/2009GL039261

Bretherton, F. P., Davis, R. E., & Fandry, C. B. (1976). A technique for objective analysis and design of oceanographic experiments. *Deep Sea Research*, 23, 559–582.

Carrillo, L., Lavín, M. F., & Palacios-Hernández, E. (2002). Seasonal evolution of the geostrophic circulation in the northern Gulf of California. *Estuarine, Coastal and Shelf Science*, 54(2), 157–173.

Carter, E. F., & Robinson, A. R. (1987). Analysis models for the estimation of oceanic fields. *Journal of Atmospheric and Oceanic Technology*, 4, 49–74.

Ciancia, E., Coviello, I., Di Polito, C., Lacava, T., Pergola, N., Satriano, V., & Tramutoli, V. (2018). Investigating the chlorophyll-a variability in the Gulf of Taranto (north-western Ionian Sea) by a multi-temporal analysis of MODIS-Aqua Level 3/Level 2 data. *Continental Shelf Research*, 155, 34–44.

Cushman-Roisin, B., Gacic, M., Poulain, P., & Artegiani, A. (2001). Physical oceanography of the Adriatic Sea: Past, present, and future, Kluwer Acad., Dordrecht, the. *Netherlands*, 304.

Demirov, E. & Pinardi, N. (2002). The Simulation of the Mediterranean Sea circulation from 1979 to 1993. Part I: The interannual variability, *Journal of Marine Systems*, 33–34, 23–50.

Devis-Morales, A., Schneider, W., Montoya-Sánchez, R. A., & Rodríguez-Rubio, E. (2008). Monsoon-like winds reverse oceanic circulation in the Panama Bight. *Geophysical Research Letters*, 35, L20607. https://doi.org/10.1029/2008GL035172

Ducet, N., Le Traon, P. Y., & Reverdin, G. (2000). Global high-resolution mapping of ocean circulation from the combination of T/P and ERS-1/2. *Journal of Geophysical Research*, 105(19), 477–498.

Eigenheer, A., & Quadfasel, D. (2000). Seasonal variability of the Bay of Bengal circulation inferred from TOPEX/Poseidon altimetry. *Journal of Geophysical Research*, 105(C2), 3243–3252.

Fang, W., Fang, G., Shi, P., Huang, Q., & Xie, Q. (2002). Seasonal structures of upper layer circulation in the southern South China Sea from in situ observations. *Journal of Geophysical Research*, 107(C11), 3202. https://doi.org/10.1029/2002JC001343

Federico, I., Pinardi, N., Coppini, G., Oddo, P., Lecci, R., & Mossa, M. (2017). Coastal ocean forecasting with an unstructured grid model in the southern Adriatic and northern Ionian seas. *Natural Hazards and Earth System Sciences*, 17, 45–59.

Frolov, S., Garau, B., & Bellingham, J. (2014). Can we do better than the grid survey: Optimal synoptic surveys in presence of variable uncertainty and decorrelation scales. *Journal of Geophysical Research: Oceans*, 119, 5071–5090. https://doi.org/10.1002/2013JC009521

Han, W., Moore, A.M., Levin, J., Zhang, B., Arango, H. G., Curchitser, E., et al. (2009). Seasonal surface ocean circulation and dynamics in the Philippine Archipelago region during 2004–2008, *Dynamics of Atmospheres and Oceans*, 47, 1–3, 114–137.

Hecht, A., Pinardi, N., & Robinson, A. R. (1998). Currents, water masses, eddies and jets in the Mediterranean Levantine Basin. *Journal of Physical Oceanography*, 18, 1320–1353.

Le Traon, P. Y., Nadal, F., & Ducet, N. (1998). An improved mapping method of multisatellite altimeter data. *Journal of Atmospheric and Oceanic Technology*, 15, 522–533.

Lermusiaux, P. F. J. (2007). Adaptive modeling, adaptive data assimilation and adaptive sampling. *Physica D*, 230, 172–196.

Liblik, T., Laanemets, J., Raudsepp, U., Elken, J., & Suhhova, I. (2013). Estuarine circulation reversals and related rapid changes in winter near-bottom oxygen conditions in the Gulf of Finland, Baltic Sea. *Ocean Science*, 9, 917–930.

Marinone, S. G. (2003). A three-dimensional model of the mean and seasonal circulation of the Gulf of California. *Journal of Geophysical Research*, *108*(C10), 3325. https://doi.org/10.1029/2002JC001720

Pinardi, N., Korres, G., Lascaratos, A., Roussenov, V., & Stanev, E. (1997). Numerical simulation of the interannual variability of the Mediterranean Sea upper ocean circulation. *Geophysical Research Letters*, *24*(4), 425–428. https://doi.org/10.1029/96GL03952

Pinardi, N., Lyubartsev, V., Cardellicchio, N., Caporale, C., Ciliberti, S., Coppini, G., et al. (2016). Marine rapid environmental assessment in the Gulf of Taranto: A multiscale approach. *Natural Hazards and Earth System Sciences*, *16*, 2623–2639. https://doi.org/10.5194/nhess-16-2623-2016

Pinardi, N., Zavatarelli, M., Adani, M., Coppini, G., Fratianni, C., Oddo, P., et al. (2015). Mediterranean Sea large-scale low frequency ocean variability and water mass formation rates from 1987 to 2007: A retrospective analysis. *Progress in Oceanography*, *132*, 318–332. https://doi.org/10.1016/j.pocean.2013.11.003

Prasad, T. G., & Ikeda, M. (2002). A numerical study of the seasonal variability of Arabian Sea high-salinity water. *Journal of Geophysical Research*, *107*(C11), 3197. https://doi.org/10.1029/2001JC001139

Preller, R. H., & Posey, P. G. (1989). A numerical model simulation of a summer reversal of the Beaufort Gyre. *Geophysical Research Letters*, *16*(1), 69–72. https://doi.org/10.1029/GL016i001p00069

Pujol, M. I., Faugère, Y., Taburet, G., Dupuy, S., Pelloquin, C., Ablain, M., & Picot, N. (2016). DUACS DT2014: The new multi-mission altimeter data set reprocessed over 20 years. *Ocean Science*, *12*, 1067–1090.

Robinson, A. R., & Sellschopp, J. (2002). Rapid assessment of the coastal ocean environment. In N. Pinardi & J. D. Woods (Eds.), *Ocean forecasting: Conceptual basis and applications* (pp. 203–232). Berlin, Heidelberg: Springer.

Rubino, A., Gačić, M., Bensi, M., Kovačević, V., Malačič, V., Menna, M., et al. (2020). Experimental evidence of long-term oceanic circulation reversals without wind influence in the North Ionian Sea, Nature. *Scientific Reports*, *10*(1), 1905. https://doi.org/10.1038/s41598-020-57862-6

Schott, F., & Fischer, J. (2000). The winter monsoon circulation of the northern Arabian Sea and Somali Current. *Journal of Geophysical Research*, *105*, 6359–6376.

Taburet, G., Sanchez-Roman, A., Ballarotta, M., Pujol, M., Legeais, J., Fournier, F., et al. (2019). Duacs dt2018: 25 years of reprocessed sea level altimetry products. *Ocean Science*, *15*, 1207–1224.

Trotta, F., Pinardi, N., Fenu, E., Grandi, A., & Lyubartsev, V. (2017). Multi-nest high-resolution model of submesoscale circulation features in the Gulf of Taranto. *Ocean Dynamics*, *67*(12), 1609–1625.

Verri, G., Pinardi, N., Oddo, P., Ciliberti, S. A., & Coppini, G. (2018). River runoff influences on the Central Mediterranean overturning circulation. *Climate Dynamics*, *50*, 1675–1703.

Wu, C. R., Shaw, P. T., & Chao, S. Y. (1998). Seasonal and interannual variations in the velocity field of the South China Sea. *Journal of Oceanography*, *54*(4), 361–372.

Yao, F., Hoteit, I., Pratt, L. J., Bower, A. S., Zhai, P., Köhl, A., & Gopalakrishnan, G. (2014a). Seasonal overturning circulation in the Red Sea: 1. Model validation and summer circulation. *Journal of Geophysical Research: Oceans*, *119*, 2238–2262. https://doi.org/10.1002/2013JC009004

Yao, F., Hoteit, I., Pratt, L. J., Bower, A. S., Zhai, P., Köhl, A., et al. (2014b). Seasonal overturning circulation in the Red Sea: 2. Winter circulation. *Journal of Geophysical Research: Oceans*, *119*, 2263–2289. https://doi.org/10.1002/2013JC009331